Supplement of

Influence of plant ecophysiology on ozone dry deposition: Comparing between multiplicative and photosynthesis-based dry deposition schemes and their responses to rising CO_2 level

Shihan Sun[1], Amos P. K. Tai[1,2], David H. Y. Yung[1], Anthony Y. H. Wong[1,3], Jason A. Ducker[4], and Christopher D. Holmes[4]

[1]Earth System Science Programme and Graduate Division of Earth and Atmospheric Sciences, Faculty of Science, The Chinese University of Hong Kong, Sha Tin, Hong Kong
[2]State Key Laboratory of Agrobiotechnology, and Institute of Environment, Energy and Sustainability, The Chinese University of Hong Kong, Sha Tin, Hong Kong
[3]Department of Earth and Environmental, Boston University, Boston, USA
[4]Department of Earth, Ocean, and Atmospheric Science, Florida State University, Tallahassee, Florida, USA

Correspondence to: Amos P. K. Tai (amostai@cuhk.edu.hk)

Content of this file

Text S1

In this study, we use four long-term measurement sites with hourly observations:

(1) The Harvard Forest Environmental Measurement Site (referred to as Harvard Forest) located in central Massachusetts. We use a O_3 EC flux dataset together with ambient O_3 concentrations (Munger and Wofsy, 1999) from year 1992 to 2006 to derive v_d. Observed ozone flux data was measured at a height of 29m at the EMS site since 1991 (dataset id: HF004). We use air density at 25ºC and 1010hPa to compute v_d when temperature measurements are missing. Observed hourly v_d values are removed if they are: (a) from days with more than 30% of missing hourly measurements are removed; (b) not fall within mean ± 3 standard deviations.

(2) The Borden Forest Research Station (referred to as Borden Forest) is located in southern Ontario, Canada. We use a database of hourly v_d from year 2008 to 2013 (Wu et al., 2016). G_s was computed using flux data from FLUXNET-Canada Dataset (TEAM, 2016). v_d values were derived with a modified gradient method (MGM) which have been proved to agree well with eddy covariance measurements. Negative v_d values and the same portion of positive v_d values with highest ranking were removed.

(3) The Blodgett Ameriflux site (referred to as Blodgett Forest) is located near Georgetown, California, US. The site is dominated by ponderosa pine, characterized by a Mediterranean climate. We use the dataset from Fare et al. (2010), which includes observed v_d and G_s from year 2001 to 2007.

(4) The SMEAR II field measurement station (System for Measuring Forest Ecosystem-Atmosphere Relationships II) is located in Hyytiälä Forest, southern Finland. We use quality-checked hourly O_3 flux and concentrations for Hyytiälä Forest from year 2007 to 2010. The height of trees near measurement tower was about 14-18m from 2000 to 2010. We use O_3 concentrations averaged from measurements at height 33.6m and 16.8m.

Text S2

The stomatal resistance parameterization for W89 is calculated as described in Wesely (1989) and Wang et al. (1998). The bulk canopy resistance is represented as:

$$R_s = r_s\left\{1+\frac{1}{[200(G+0.1)]^2}\right\}\left\{\frac{400}{T_s(40-T_s)}\right\}D_i/D_v],$$

where G is solar radiation, T_s is surface air temperature. D_i and D_v are molecular diffusivities for water and the pollutant gas respectively.

The stomatal resistance parameterization for Z03 is calculated as described in Zhang et al. (2003) and Zhang et al. (2002). The expressions to calculate stomatal conductance implemented in TEMIR are also represented here.

$$R_s = 1/[G_s(\mathrm{PAR})f(T)f(\mathrm{VPD})f(\psi)D_i/D_v],$$

where $f(T)$, $f(\mathrm{VPD})$ and $f(\psi)$ are dimensionless stress functions for temperature (T), vapor pressure deficit (VPD), and water stress (ψ) respectively as described in Brook et al. (1999). $G_s(\mathrm{PAR})$ is the unstressed canopy stomatal conductance. G_s is calculated as weighted sum of sunlit and shaded leaves.

$$G_s(\mathrm{LAI},\mathrm{PAR}) = L_{sun}/r_s(\mathrm{PAR}_{sun}) + L_{sha}/r_s(\mathrm{PAR}_{sha}),$$

$$r_s(\mathrm{PAR}) = r_{smin}(1+b_{rs}/\mathrm{PAR}),$$

where L_{sun} and L_{sha} are total sunlit and shaded leaf area index (LAI), PAR_{sun} and PAR_{sha} are absorbed *PAR* averaged over sunlit and shaded leaves, r_{smin} and b_{rs} are minimum stomatal resistance and empirical light response constant for stomatal resistance. The expression for PAR_{sun} and PAR_{sha} as expressed follows. For LAI < 2.5 or solar radiation < 200 $\mathrm{Wm^{-2}}$:

$$\mathrm{PAR}_{sha} = R_{diff}e^{-0.5\mathrm{LAI}^{0.7}} + 0.07R_{dir}\times(1.1-0.1\mathrm{LAI})e^{-\cos\theta},$$

$$\mathrm{PAR}_{sun} = \mathrm{PAR}_{sha} + R_{dir}\cos\alpha/\cos\theta,$$

For the other conditions:

$$\mathrm{PAR}_{sha} = R_{diff}e^{-0.5\mathrm{LAI}^{0.8}} + 0.07R_{dir}\times(1.1-0.1\mathrm{LAI})e^{-\cos\theta},$$

$$\mathrm{PAR}_{sun} = \mathrm{PAR}_{sha} + R_{dir}^{0.8}\cos\alpha/\cos\theta,$$

where α is the angle between the leaf and the sun, θ is the solar zenith angle, R_{diff} and R_{dir} are the downward visible radiation fluxes from diffuse and direct-beam radiation above the canopy.

$$f(T) = \left[(T-T_{min})/(T_{opt}-T_{min})\right]\times\left[(T_{max}-T)/(T_{max}-T_{opt})\right]^{bt},$$

$$bt = \left[(T_{max}-T_{opt})/(T_{opt}-T_{min})\right],$$

where T_{min}, T_{max}, T_{opt} are minimum, maximum and optimum temperature respectively.

$$f(D) = 1-b_{vpd}D,$$

where b_{vpd} and D are vapour pressure constant and vapour pressure deficit.

$$f(\psi) = (\psi-\psi_{c2})/(\psi_{c1}-\psi_{c2}),$$

$$\psi = -0.72-0.0013\mathrm{SR},$$

where ψ_{c1} and ψ_{c2} are parameters tat specify leaf water potential dependency, SR is solar radiation.

For the photosynthesis-stomatal conductance module in TEMIR, we follow the description by the Community Land Model 4.5 (CLM4.5) (Oleson et al., 2013). A brief summary is also represented here. Photosynthesis in C3 and C4 plants is computed as follows based on Collatz et al. (1992):

$$A_{\mathrm{n}} = \min\left(A_{\mathrm{c}}, A_{\mathrm{j}}, A_{\mathrm{p}}\right) - R_{\mathrm{d}},$$

The Rubisco-limited photosynthetic rate (A_c, μmol $m^{-2}s^{-1}$) is:

$$A_{\mathrm{c}} = \begin{cases} V_{\mathrm{cmax}} * \frac{c_{\mathrm{i}} - \Gamma_*}{c_{\mathrm{i}} + K_{\mathrm{c}} * \left(1 + \frac{o_{\mathrm{i}}}{K_{\mathrm{o}}}\right)} & \text{for C3 plants} \\ V_{\mathrm{cmax}} & \text{for C4 plants} \end{cases},$$

The RuBP-limited photosynthetic rate (A_j, μmol $m^{-2}s^{-1}$) is:

$$A_{\mathrm{j}} = \begin{cases} \frac{J}{4} * \frac{c_{\mathrm{i}} - \Gamma_*}{c_{\mathrm{i}} + 2\Gamma_*} & \text{for C3 plants} \\ 2.3 * \varphi & \text{for C4 plants} \end{cases},$$

The product-limited photosynthetic rate (A_p, μmol $m^{-2}s^{-1}$) is:

$$A_{\mathrm{p}} = \begin{cases} 3 * T_{\mathrm{p}} & \text{for C3 plants} \\ k_p * \frac{c_{\mathrm{i}}}{P_{\mathrm{atm}}} & \text{for C4 plants} \end{cases},$$

The dark respiration (R_d, μmol $m^{-2}s^{-1}$), which is adjusted by the water stress factor β_t, is given by:

$$R_{\mathrm{d}} = \begin{cases} 0.015 * V_{\mathrm{cmax}} * \beta_{\mathrm{t}} & \text{for C3 plants} \\ 0.025 * V_{\mathrm{cmax}} * \beta_{\mathrm{t}} & \text{for C4 plants} \end{cases}$$

In the equations above, c_i is the intercellular CO_2 partial pressure (Pa). K_c and K_o are the Michaelis–Menten constants for carboxylation and oxygenation (Pa). o_i is the intercellular oxygen partial pressure (Pa). Γ_* is the CO_2 compensation point (Pa). V_{cmax} is the maximum rate of carboxylation (μmol m^{-2} s^{-1}). φ is the absorbed PAR (μmol m^{-2} s^{-1}). J is the electron transport rate (μmol $m^{-2}s^{-1}$). T_p is the triose phosphate utilization rate (μmol m^{-2} s^{-1}), P_{atm} is the ambient atmospheric pressure (Pa), k_p is the initial slope of CO_2 response curve for C4 plants (Pa / Pa). The function β_t ranges from one when soil is wet and to zero when soil is dry.

The stomatal conductance of water g_s (μmol $m^{-2}s^{-1}$) for FBB and MED is then calculated as in Eq. (4) and Eq. (5) in the main text.

Table S1. References of observational datasets.

Land type group	Lat	Lon	Site	LAI	Canopy Height (m)	Sampling Period	Reference
Deciduous Forest	42.7ºN	72.2ºW	Harvard Forest	3.4	24	Jan 1991~Dec 1994	Munger et al. (1996)
	42.7ºN	72.2ºW	Harvard Forest	3.4	24	Jun-Nov, 2000	Wu et al. (2011)
	41.56ºN	78.77ºW	Kane Experimental Forest, Pennsylvania	1-7	22-23	Apr 29, 1997~Oct 23, 1997	Finkelstein et al. (2000)
	44.3ºN	79.9ºW	Borden Forest, Ontario, Canada	2.3-4.5	22	01 May, 2008-30 Apr, 2013	Wu et al. (2018)
	44.3ºN	80.9ºW	Borden Forest, Ontario, Canada	6	18	Aug 2-3, 1988	Padro et al. (1991)
	44.3ºN	80.9ºW	Borden Forest, Ontario, Canada	0.5	18	Mar 17~Apr 26, 1990	Padro et al. (1992)
	18.3ºN	99.7ºE	Teak forest in Mea Moh, Thailand	\	12	Jan-Apr 2002	Matsuda et al. (2005)
	18.3ºN	99.7ºE	Teak forest in Mea Moh, Thailand	\	12	Jan-Aug, 2004	Matsuda et al. (2006)
	51.17ºN	0.84ºW	Alice Holt, England	\	13	Jul 16 – Aug 18, 2005	Fowler et al. (2009)
	41.7ºN	12.35ºE	Castelporziano, Italy	3.7	19.7	2012-2013	Fares et al. (2014)
Coniferous Forest	38.9ºN	120.6ºW	Blodgett Forest, California	3.6	5	Jun 1999~Jun 2000	Kurpius et al. (2002)
	56.3ºN	8.4ºE	Ulborg Forest, Denmark	8	12	Jun 1994, Sep 1995	Mikkelsen et al. (2000)
	56.3ºN	8.4ºE	Ulborg Forest, Denmark	8	12	Jan 1996~Dec 2000	Mikkelsen et al. (2004)
	54.8ºN	66.9ºW	Schefferville, Canada	\	5-6	Jun-Aug 1990	Munger et al. (1996)
	40.0ºN	105.5ºW	Niwot Ridge AmeriFlux site, Colorado	4.2	11.4	Jun-Aug 2002; May-Sep, 2003; May-Aug, 2005	Turnipseed et al. (2009)
	55.3ºN	-3.4ºW	Rivox Forest, Scotland	10.2	13	May 23-27, 1992	Coe et al. (1995)
	61.85ºN	24.28ºE	Hyytiälä, Southern Finland	6	14-18	Aug 2001-Dec 2010	Rannik et al. (2012)
	35.97ºN	79.13ºW	Blackwood division of Duke forest	3.1	14	Apr 15-May 15 1996	Finkelstein et al. (2000)
	60.4ºN	11.1ºE	Hurdal, South-East Norway	3.4-4.5	13	Jul 1, 2000-Mar 31, 2003	Hole et al. (2004)
	38.9ºN	120.6ºW	Blodgett Forest	1.2-2.9	4-7.6	2001-2006	Fares et al. (2010)
	44.2ºN	0.7ºW	Pine forest in southwestern France	3	15	Jun 9-22, 1992	Lamaud et al. (1994)
	44.2ºN	0.7ºW	Pine forest in southwestern France	2.1	16~24	Jun 21-Jul 3, 1994; Feb 21-Mar 24, 1997	Lamaud et al. (2002)
Grass	55.79ºN	3.24ºW	Auchencorth Moss	\	1	Jan 1995~Dec 1998	Fowler et al. (2001)

	40.7ºN	8.6ºW	Polder Piolto de Sarrazola	2.5-4.5	0.1-0.8	Nov 1994~Oct 1995	Pio et al. (2000)
	37ºN	119.8ºW	Fresno, California	1	0.2	Jul 8~Aug 6, 1991	Padro et al. (1994)
	10.75ºS	62.37ºW	Rondonia, Brazil	3.9	\	Jan-Feb, 1999	Sigler et al. (2002)
	45.8ºN	8.63ºE	Ispra, Italy	\	0.25	Sep 16–23, 1997	Cieslik (2004)
	48.17ºN	8.75ºE	Klippeneck, Germany	\	0.2	Sep10-22, 1992	Cieslik (2004)
	40.1ºN	88.2ºW	Champaign, Illinois	\	0.25-0.3	Jun 26-27, 1982	Droppo et al. (1985)
	34.29ºN	85.97ºW	Crossvile, Alabama	1-2.3	0.1-0.3	Apr 15-Jun13, 1995	Meyers et al. (1998)
Crop	36.8ºN	120.7ºW	Fresno, California	1.8-2.7	0.4-0.9	Jul 8~Aug 6, 1991	Padro et al. (1994)
	48.7ºN	8ºE	Scherzheim, Denmark	\	\	Sep 11-22, 1992	Pilegaard et al. (1998)
	48.85ºN	1.97ºE	Grignon, France	5.2	2.2	Apr 28, 2008~Sep 9, 2008	Stella et al. (2011)
	44.4ºN	0.63ºW	La Cape Sud, France	5.1	2.5	Jul 2007–Oct 2007	Stella et al. (2011)
	43.82ºN	1.38ºE	Lamasquere, France	3.2	2.5	May 2008–Sep 2008	Stella et al. (2011)
	40.05ºN	88.37ºW	Bondville, Illinois	2.5-3.3	1.8-2.4	Aug 18-Oct 1, 1994	Meyers et al. (1998)
	36.65ºN	87.03ºW	Nashville, Tennessee	1~6	1.2	Jun 22-Oct 11, 1995	Meyers et al. (1998)
	55.9ºN	2.8ºW	Gilchriston Farm, Scotland	3	0.3	Jul, 2006	Coyle et al. (2009)
Rainforest	4.97ºN	117.85ºE	Bukit Atur near Danum Valley	6	30	Apr-Jul, 2008	Fowler et al. (2011)
	10.08ºS	61.93ºW	Reserva Biologica Juru, Brazil	5.6	40	May 4-22, Sep 21-Oct 20, 1999	Rummel et al. (2007)
	3ºS	59.9ºW	Reserva Florestal Ducke	7	30	Apr 22-May 8, 1987	Fan et al. (1990)

Table S2. Statistic summary of meteorological variables at long-term sites. Precip: liquid precipitation (kg m^{-2} s^{-1}); Temp: surface temperature (ºC); GWR: root zone soil wetness; SWGDN: short wave radiation (W m^{-2}); VPD: vapor pressure deficit (kPa); RH: relative humidity.

	Harvard Forest		**Blodgett Forest**		**Hyytiälä Forest**		**Borden Forest**	
Season	DJF	JJA	DJF	JJA	DJF	JJA	DJF	JJA
Precip	0.06	0.05	0.07	0.00	0.01	0.01	0.00	0.00
Temp	-2.3	18.6	4.3	19.6	-5.1	15.3	-4.4	19.9
GWR	0.58	0.38	0.42	0.26	0.62	0.60	0.669	0.50
SWGDN	72	225	97	343	11	191	64	273
RH	0.82	0.84	0.66	0.42	0.91	0.74	0.92	0.75
VPD	0.09	0.38	0.29	1.39	0.04	0.49	0.04	0.67

Table S3. PFT and land category mapping among CLM, Z03 and W89.

CLM PFT	Z03 surface type	W89 surface type
Needleleaf evergreen tree - temperate	Evergreen needleleaf trees	Coniferous forest
Needleleaf evergreen tree - boreal		
Needleleaf deciduous tree - boreal	Deciduous needleleaf trees	
Broadleaf evergreen tree - tropical	Tropical broadleaf trees	Amazon forest
Broadleaf deciduous tree - tropical	Deciduous broadleaf trees	Deciduous forest
Broadleaf deciduous tree - temperate		
Broadleaf deciduous tree - boreal		
Broadleaf evergreen shrub - temperate	Thorn shrubs	Shrub/grassland
Broadleaf deciduous shrub - temperate	Deciduous shrubs	
Broadleaf deciduous shrub - boreal		
C_3 arctic grass	Tundra	Tundra
C_3 non-arctic grass	Short grass	Shrub/grassland
C_4 grass	Corn	
C_3 crop	Crops	Agricultural land
C_3 irrigated		

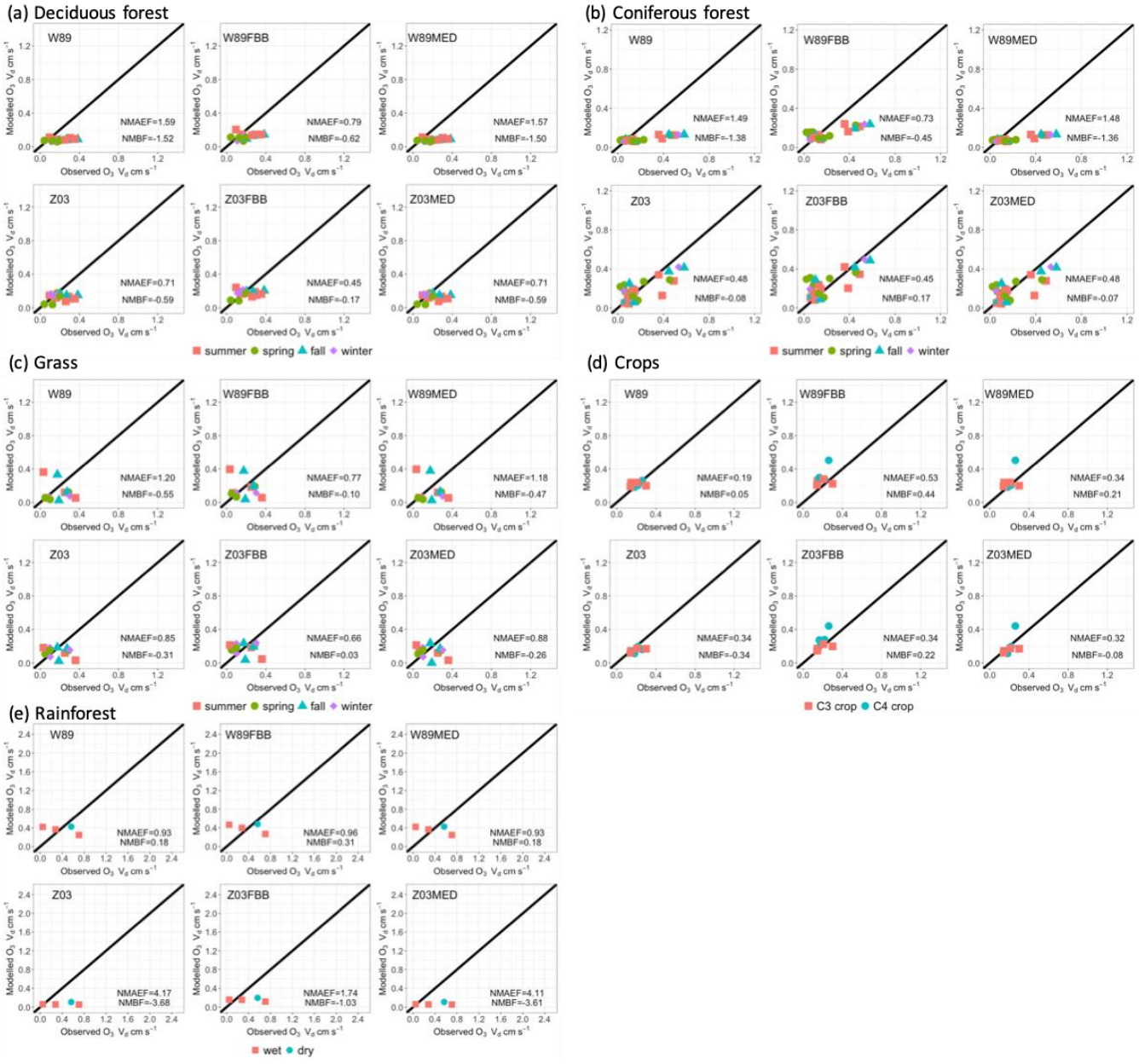

Figure S1. Average nighttime (LT 22:00pm~4:00am) observed-simulated dry deposition velocities for five land types. Colours indicate dominant seasons during field measurements, except that for crops different colours indicate crop types (C3 and C4 crops).

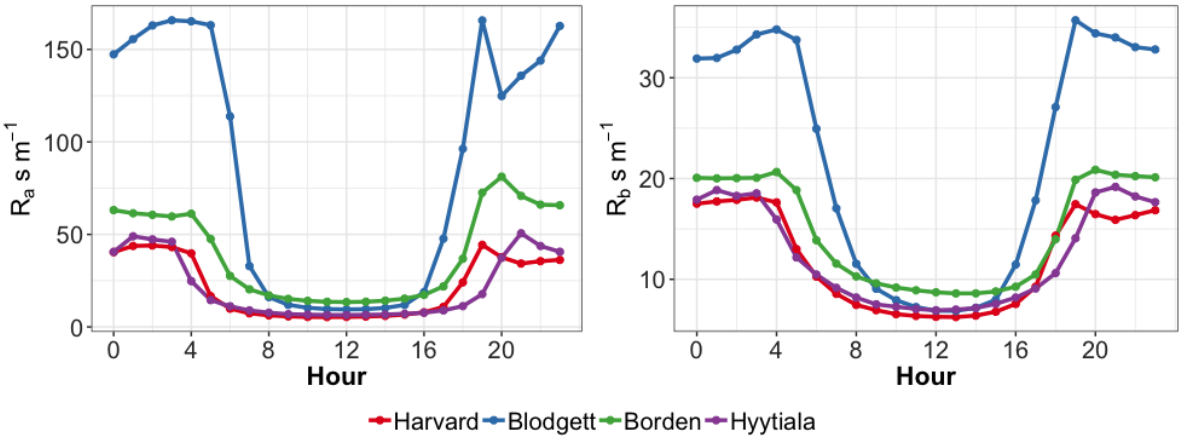

Figure S2. Average JJA diurnal aerodynamic resistance (R_a) and boundary layer resistance (R_b) at long-term measurement sites.

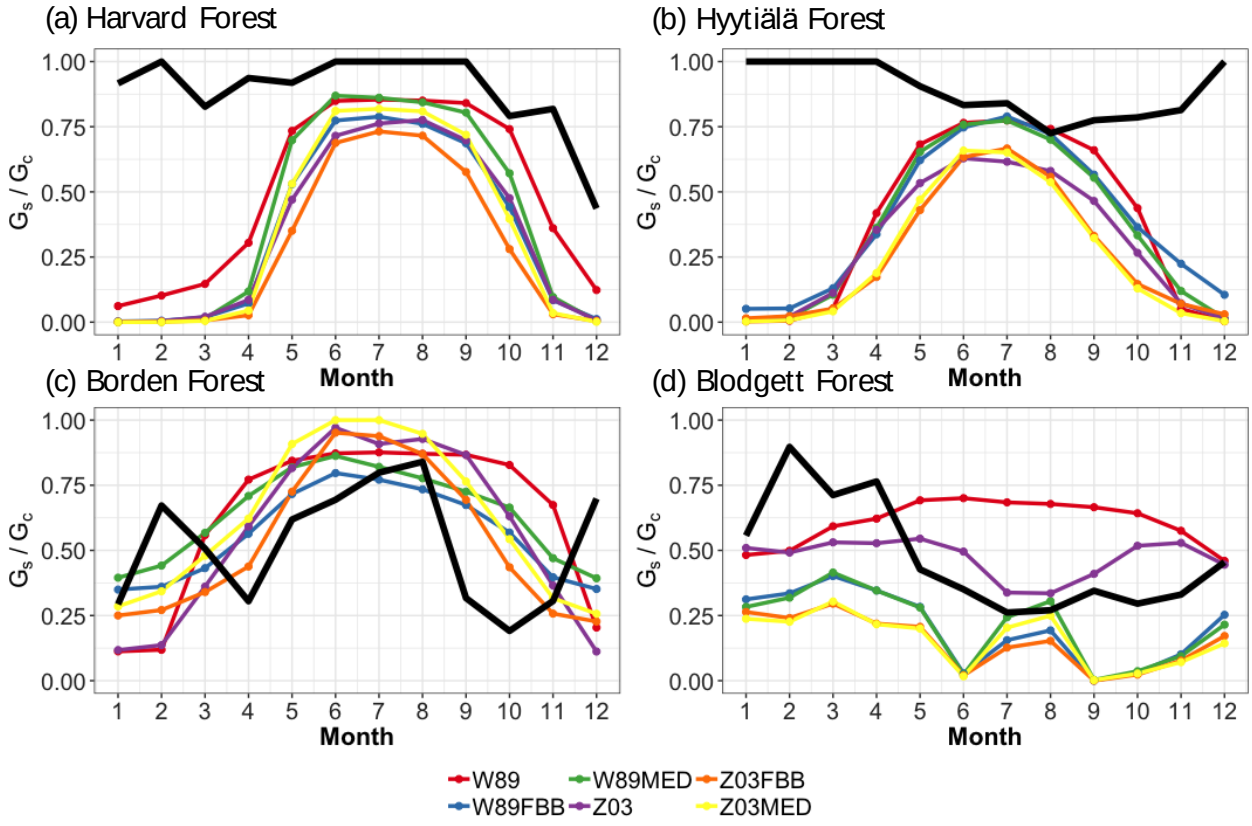

Figure S3. Fraction of average monthly daytime stomatal conductance to canopy conductance (G_s/G_c) at long-term measurement sites.

References in the Supplementary

Cieslik, S. A.: Ozone uptake by various surface types: a comparison between dose and exposure, Atmos. Environ., 38, 2409-2420, https://doi.org/10.1016/j.atmosenv.2003.10.063, 2004.

Coe, H., Gallagher, M. W., Choularton, T. W., and Dore, C.: Canopy Scale Measurements of Stomatal and Cuticular O3 Uptake by Sitka Spruce, Atmos. Environ., 29, 1413-1423, https://doi.org/10.1016/1352-2310(95)00034-V, 1995.

Collatz, G. J., Ribas-Carbo, M., and Berry, J. A.: Coupled Photosynthesis-Stomatal Conductance Model for Leaves of C4 Plants, Aust. J. Plant Physiol., 19, 519-538, https://doi.org/10.1071/Pp9920519, 1992.

Coyle, M., Nemitz, E., Storeton-West, R., Fowler, D., and Cape, J. N.: Measurements of ozone deposition to a potato canopy, Agr. Forest Meteorol., 149, 655-666, https://doi.org/10.1016/j.agrformet.2008.10.020, 2009.

Fan, S. M., Wofsy, S. C., Bakwin, P. S., Jacob, D. J., and Fitzjarrald, D. R.: Atmosphere-Biosphere Exchange of CO_2 and O_3 in the Central Amazon Forest, J. Geophys. Res.-Atmos., 95, 16851-16864, https://doi.org/10.1029/JD095iD10p16851, 1990.

Finkelstein, P. L., Ellestad, T. G., Clarke, J. F., Meyers, T. P., Schwede, D. B., Hebert, E. O., and Neal, J. A.: Ozone and sulfur dioxide dry deposition to forests: Observations and model evaluation, J. Geophys. Res.-Atmos., 105, 15365-15377, https://doi.org/10.1029/2000jd900185, 2000.

Fowler, D., Flechard, C., Cape, J. N., Storeton-West, R. L., and Coyle, M.: Measurements of ozone deposition to vegetation quantifying the flux, the stomatal and non-stomatal components, Water Air Soil Poll., 130, 63-74, https://doi.org/10.1023/A:1012243317471, 2001.

Fowler, D., Nemitz, E., Misztal, P., Di Marco, C., Skiba, U., Ryder, J., Helfter, C., Cape, J. N., Owen, S., Dorsey, J., Gallagher, M. W., Coyle, M., Phillips, G., Davison, B., Langford, B., MacKenzie, R., Muller, J., Siong, J., Dari-Salisburgo, C., Di Carlo, P., Aruffo, E., Giammaria, F., Pyle, J. A., and Hewitt, C. N.: Effects of land use on surface-atmosphere exchanges of trace gases and energy in Borneo: comparing fluxes over oil palm plantations and a rainforest, Philos. T. R. Soc. B., 366, 3196-3209, https://doi.org/10.1098/rstb.2011.0055, 2011.

Kurpius, M. R., McKay, M., and Goldstein, A. H.: Annual ozone deposition to a Sierra Nevada ponderosa pine plantation, Atmos. Environ., 36, 4503-4515, https://doi.org/10.1016/S1352-2310(02)00423-5, 2002.

Lamaud, E., Brunet, Y., Labatut, A., Lopez, A., Fontan, J., Druilhet, A.: The Landes experiment: biosphere–atmosphere exchanges of ozone and aerosol particles above a pine forest. J. Geophys. Res., 99, 16511–16521, https://doi.org/10.1029/94JD00668, 1994.

Lamaud, E., Carrara, A., Brunet, Y., López, A., & Druilhet, A.: Ozone fluxes above and within a pine forest canopy in dry and wet conditions. Atmos. Environ., 36, 77–88, https://doi.org/10.1016/S1352-2310(01)00468-X, 2002.

Meyers, T. P., Finkelstein, P., Clarke, J., Ellestad, T. G., and Sims, P. F.: A multilayer model for inferring dry deposition using standard meteorological measurements, J. Geophys. Res.-Atmos., 103, 22645-22661, https://doi.org/10.1029/98jd01564, 1998.

Mikkelsen, T. N., Ro-Poulsen, H., Pilegaard, K., Hovmand, M. F., Jensen, N. O., Christensen, C. S., and Hummelshoej, P.: Ozone uptake by an evergreen forest canopy: temporal variation and possible mechanisms, Environ. Pollut., 109, 423-429, https://doi.org/10.1016/S0269-7491(00)00045-2, 2000.

Munger, J. W., Wofsy, S. C., Bakwin, P. S., Fan, S. M., Goulden, M. L., Daube, B. C., Goldstein, A. H., Moore, K. E., and Fitzjarrald, D. R.: Atmospheric deposition of reactive nitrogen oxides and ozone in a temperate deciduous forest and a subarctic woodland .1. Measurements and mechanisms, J. Geophys. Res.-Atmos., 101, 12639-12657, https://doi.org/10.1029/96jd00230, 1996.

Munger, W., and Wofsy, S.: Canopy-atmosphere exchange of carbon, water and energy at Harvard Forest EMS Tower since 1991, Harvard Forest Data Archive: HF004, 1999.

Oleson, K., Lawrence, D., Bonan, G., Drewniak, B., Huang, M., Koven, C., Levis, S., Li, F., Riley, W., and Subin, Z.: Technical description of version 4.5 of the Community Land Model (CLM), NCAR Technical Note: NCAR/TN-503+ STR, National Center for Atmospheric Research (NCAR), Boulder, CO, USA, https://doi.org/10.5065/D6RR1W7M, 2013.

Padro, J., Massman, W. J., Shaw, R. H., Delany, A., and Oncley, S. P.: A Comparison of Some Aerodynamic Resistance Methods Using Measurements over Cotton and Grass from the 1991 California Ozone Deposition Experiment, Bound.-Lay. Meteorol., 71, 327-339, https://doi.org/10.1007/Bf00712174, 1994.

Pilegaard, K., Hummelshoj, P., and Jensen, N. O.: Fluxes of ozone and nitrogen dioxide measured by eddy correlation over a harvested wheat field, Atmos. Environ., 32, 1167-1177, https://doi.org/10.1016/S1352-2310(97)00194-5, 1998.

Pio, C. A., Feliciano, M. S., Vermeulen, A. T., and Sousa, E. C.: Seasonal variability of ozone dry deposition under southern European climate conditions, in Portugal, Atmos. Environ., 34, 195-205, https://doi.org/10.1016/S1352-2310(99)00276-9, 2000.

Rannik, U., Altimir, N., Mammarella, I., Back, J., Rinne, J., Ruuskanen, T. M., Hari, P., Vesala, T., and Kulmala, M.: Ozone deposition into a boreal forest over a decade of observations: evaluating deposition partitioning and driving variables, Atmos. Chem. Phys., 12, 12165-12182, https://doi.org/10.5194/acp-12-12165-2012, 2012.

Rummel, U., Ammann, C., Kirkman, G. A., Moura, M. A. L., Foken, T., Andreae, M. O., and Meixner, F. X.: Seasonal variation of ozone deposition to a tropical rain forest in southwest Amazonia, Atmos. Chem. Phys., 7, 5415-5435, https://doi.org/10.5194/acp-7-5415-2007, 2007.

Sigler, J. M., Fuentes, J. D., Heitz, R. C., Garstang, M., and Fisch, G.: Ozone dynamics and deposition processes at a deforested site in the Amazon Basin, Ambio., 31, 21-27, https://doi.org/10.1579/0044-7447-31.1.21, 2002.

Stella, P., Personne, E., Loubet, B., Lamaud, E., Ceschia, E., Beziat, P., Bonnefond, J. M., Irvine, M., Keravec, P., Mascher, N., and Cellier, P.: Predicting and partitioning ozone fluxes to maize crops from sowing to harvest: the Surfatm-O_3 model, Biogeosciences, 8, 2869-2886, https://doi.org/10.5194/bg-8-2869-2011, 2011.

TEAM, F. C.: FLUXNET Canada Research Network-Canadian Carbon Program Data Collection, 1993-2014, ORNL DAAC, 2016.

Turnipseed, A. A., Burns, S. P., Moore, D. J. P., Hu, J., Guenther, A. B., and Monson, R. K.: Controls over ozone deposition to a high elevation subalpine forest, Agr. Forest Meteorol., 149, 1447-1459, https://doi.org/10.1016/j.agrformet.2009.04.001, 2009.

Wu, Z. Y., Wang, X. M., Chen, F., Turnipseed, A. A., Guenther, A. B., Niyogi, D., Charusombat, U., Xia, B. C., Munger, J. W., and Alapaty, K.: Evaluating the calculated dry deposition velocities of reactive nitrogen oxides and ozone from two community models over a temperate deciduous forest, Atmos. Environ., 45, 2663-2674, https://doi.org/10.1016/j.atmosenv.2011.02.063, 2011.

Wu, Z. Y., Staebler, R., Vet, R., and Zhang, L. M.: Dry deposition of O_3 and SO_2 estimated from gradient measurements above a temperate mixed forest, Environ. Pollut., 210, 202-210, https://doi.org/10.1016/j.envpol.2015.11.052, 2016.

Wu, Z. Y., Schwede, D. B., Vet, R., Walker, J. T., Shaw, M., Staebler, R., and Zhang, L. M.: Evaluation and Intercomparison of Five North American Dry Deposition Algorithms at a Mixed Forest Site, J. Adv. Model Earth Sy., 10, 1571-1586, https://doi.org/10.1029/2017ms001231, 2018.

Zhang, L. M., Moran, M. D., Makar, P. A., Brook, J. R., and Gong, S. L.: Modelling gaseous dry deposition in AURAMS: a unified regional air-quality modelling system, Atmos. Environ., 36, 537-560, https://doi.org/10.1016/S1352-2310(01)00447-2, 2002.

Zhang, L., Brook, J. R., and Vet, R.: A revised parameterization for gaseous dry deposition in air-quality models, Atmos. Chem. Phys., 3, 2067-2082, https://doi.org/10.5194/acp-3-2067-2003, 2003.